FLOW SEPARATION NOISE SOURCES

Alexandre Suryadi and Michaela Herr

Dept. Wind Energy, German Aerospace Center (DLR)

Braunschweig

DLR

Outline

- Introduction
- Experimental setup
- Coherent Output Power
- Results
- Conclusions

Introduction

- Wind turbine under heavy load is susceptible to flow separation due to gusts or other unfavorable atmospheric conditions.
- Flow separation reduces lift and increases drag considerably
  - → loss of power generation
  - → Increase noise emission and immision
- Blade pitch control to mitigate flow separation
  - ? Detection of flow separation: breathing phenomena, vortex shedding frequency, etc.
  - ? Optimize detection and control
  - ? Noise penalty
- Motivation: classify the noise sources of flow separation for a better understanding of flow separation noise

Experimental Setup

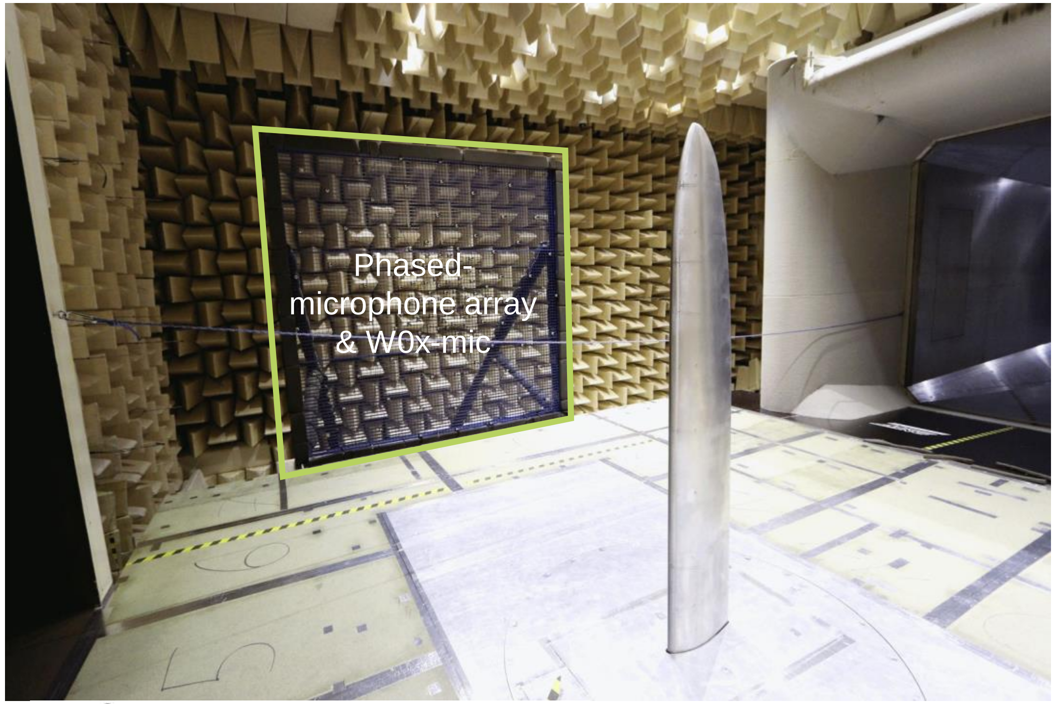

- Low-speed Wind Tunnel Braunschweig (NWB)
- ¾-open anechoic test section (rated for f>100 Hz)
- U_0= 52, 60, 70, 80 m/s (Re= 1.16 – 1.9 M, Ma= 0.15-0.24)
- NACA 64-618 Blade tip model, b=2.1 m, $\bar{c}_a$= 326 mm
- α= 0° – 21°

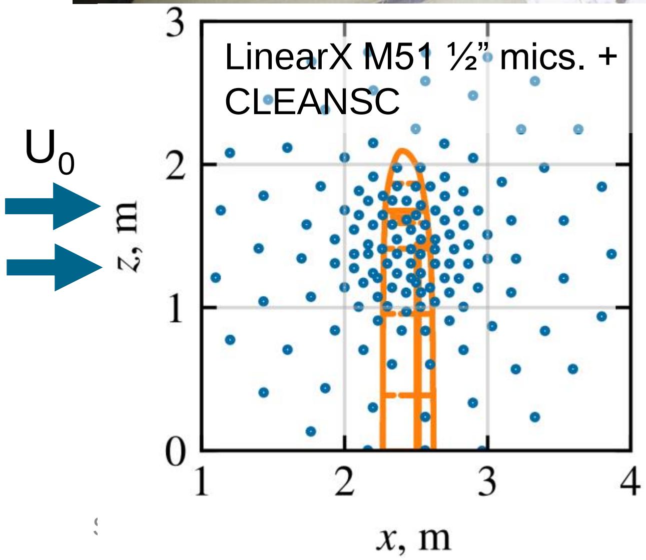

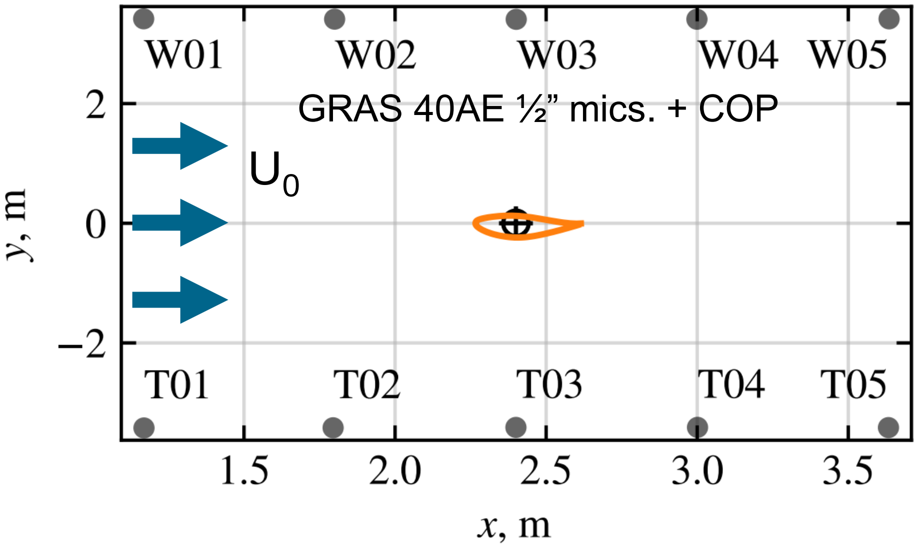

T= 30 s
SR= 100 kHz

Additional instrumentations:
- 4 Kulite ultraminiature surface pressure sensor along the trailing edge

Coherent Output Power (COP)

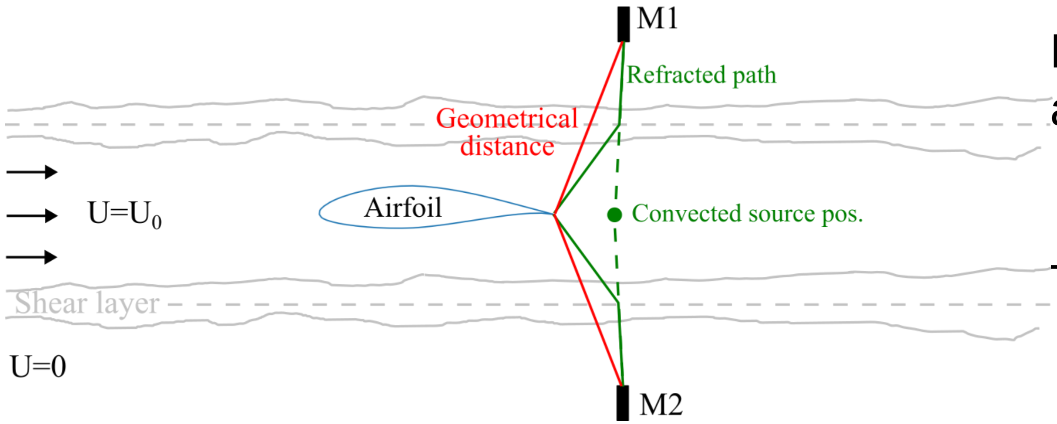

Edge radiated noise (dipole sound source) that arrive at M1 and M2 is coherent and has an anti-symmetric phase angle

$$\gamma_{12} > 0; \theta_{12} = \pm\pi$$

The noise that arrive at each microphone,

$$p' = p'^{(a)} + n$$

Power spectral densities of M1 and M2,

$$\phi_{11} = \phi_{11}^{(a)} + \phi_{n1};\ \phi_{22} = \phi_{22}^{(a)} + \phi_{n2}$$

The cross-spectral density between M1 and M2,

$$|\phi_{12}| = \left|\phi_{12}^{(a)}\right| \approx \phi_{11}^{(a)} \approx \phi_{22}^{(a)}$$

Given incoherent $p'^{(a)}$ and n and incoherent n_1 and n_2, between M1 and M2

Brooks & Hodgson, 1981 Trailing Edge Noise Prediction From Measured Surface Pressure

Results

Aerodynamics

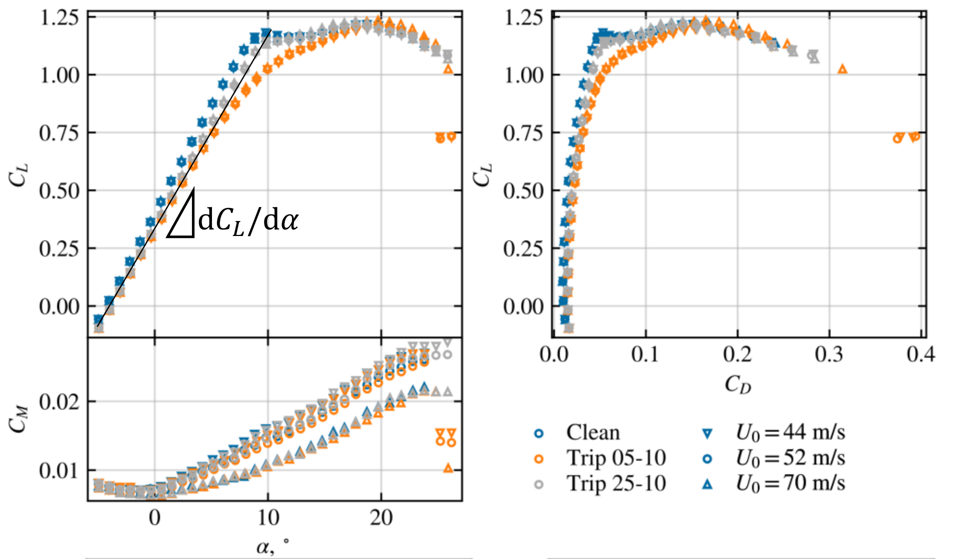

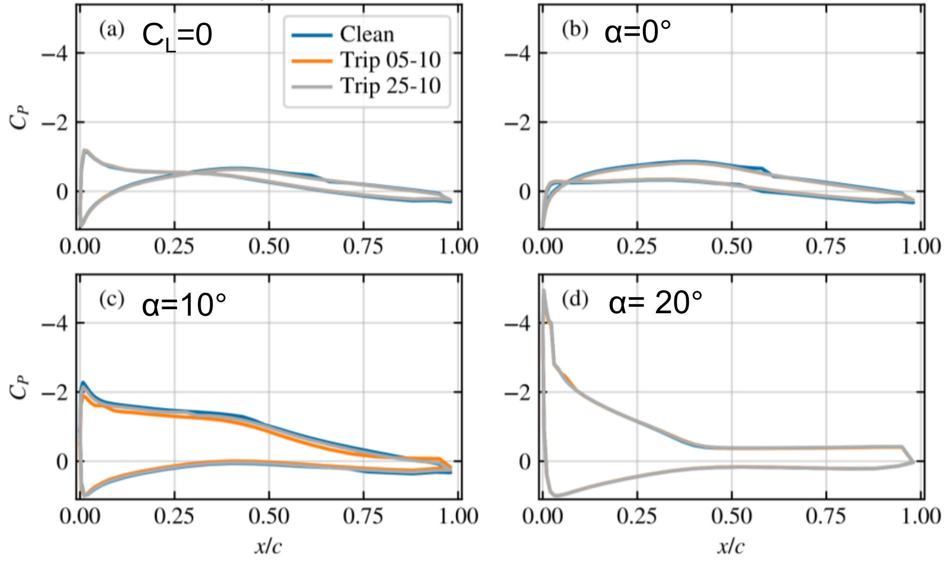

- Trip 05-10: Zig zag strips: 0.4 mm
  - 5%c on the suction side
  - 10%c on the pressure side
- Stall at α= 20°
- Deviation from the linear slope at α= 7°
- Lift plateau avoided at 10°<α<15°

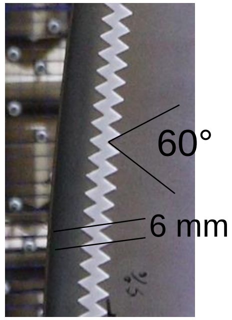

At α=10°, smaller C_P on the suction side, consistent with the smaller C_L

~ 60%c separated region at α= 20°

Results

Coherent Output Power

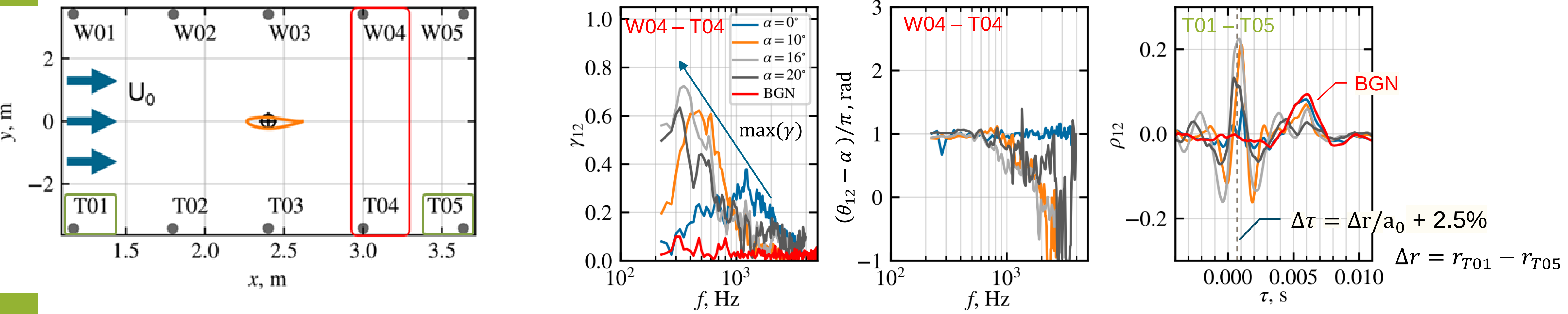

- The test section's shear layer has zero coherence.
- α= 0°: max coherence at f>1 kHz
- Larger α: max coherence increases and shifts to lower frequency.
- The phase angle compensated for α ≈ π.
  - The frequency range decreases with increasing α. To impose anti-symmetry, we use the co-spectrum, i.e. $|\phi_{12}| = \mathrm{Re}(\phi_{12})$
- Cross-correlation shows that the measured signal is mostly from the trailing edge

Results

Source Localization, α= 0°

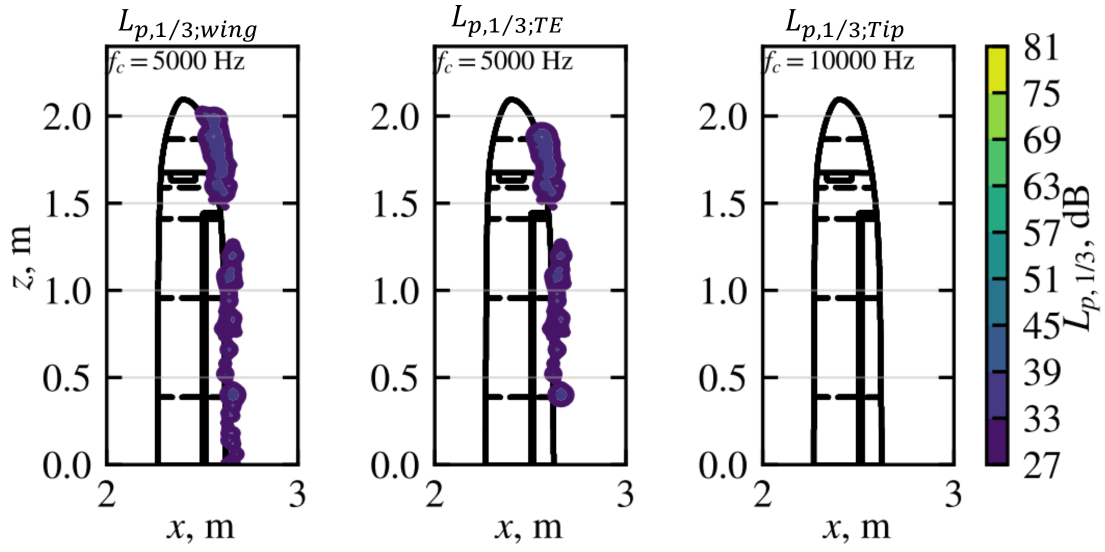

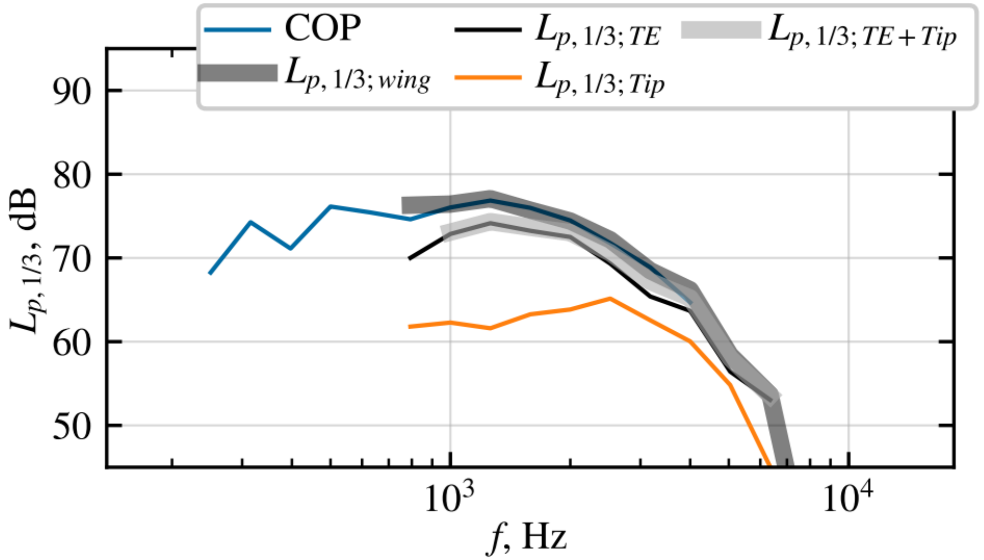

- The sound source is predominantly from the trailing edge.
- No tip noise.
- COP spectrum = Array + 4dB.
  - Given only trailing-edge noise sources, COP $\approx L_{p,1/3;wing}$.
- $L_{p,1/3;wing} = L_{p,1/3;TE} + 2\text{dB}$, because of the different integrated span lengths.

Results

Source Localization, α= 10°

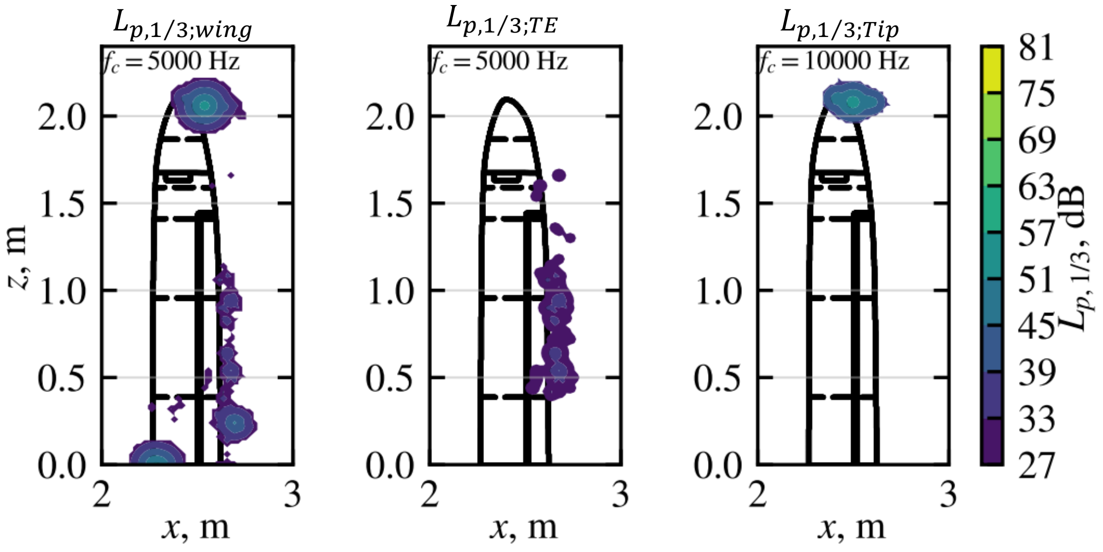

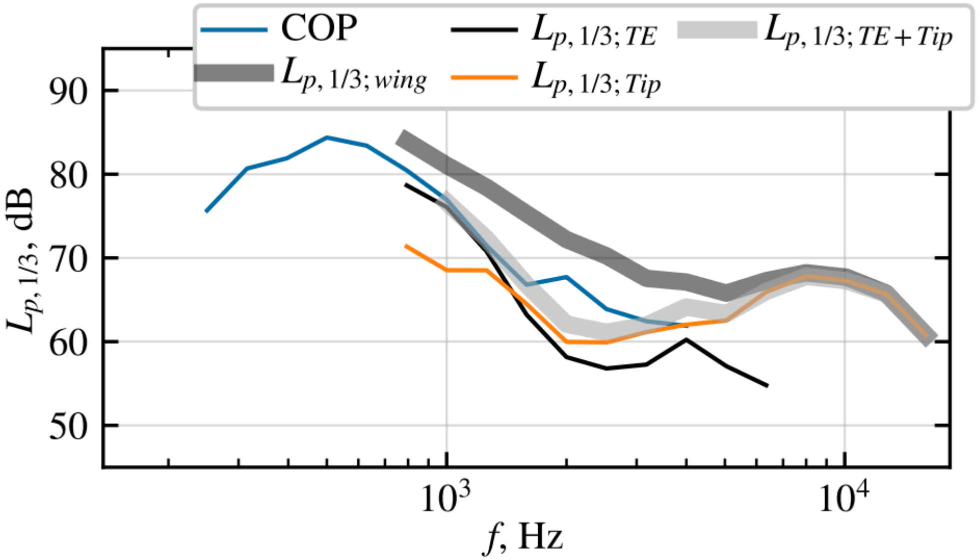

- $L_{p,1/3;Tip}$ and installation noise is non-negligible.
- $L_{p,1/3;Tip}$ is predominant at high frequency and has a maximum at 8 kHz.
- $L_{p,1/3;TE}$ is weaker compared with α=0°.
- COP spectrum is maximum at 500 Hz.

Results

Source Localization, α= 16°

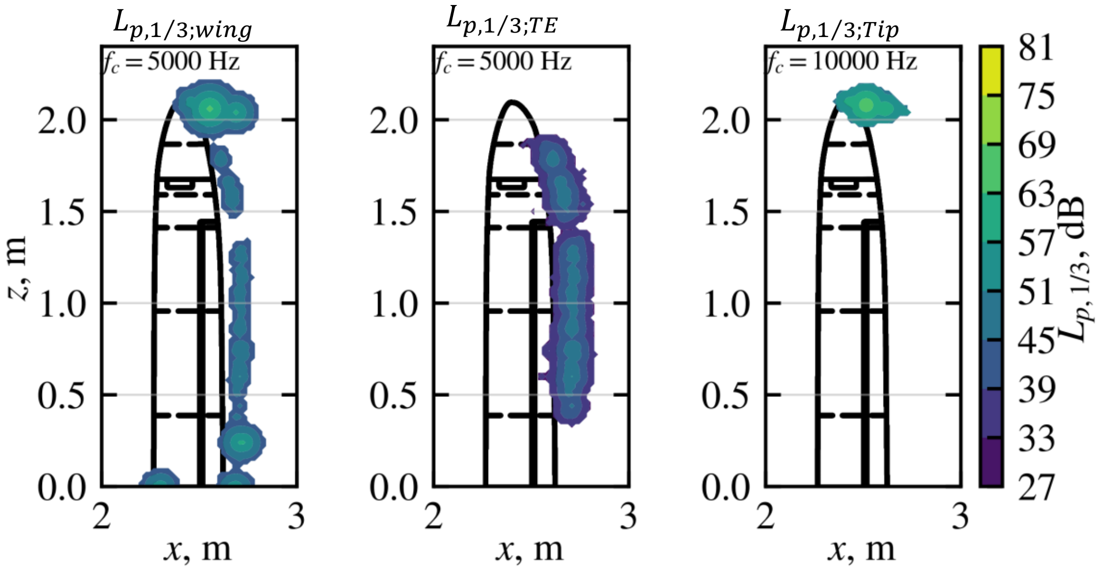

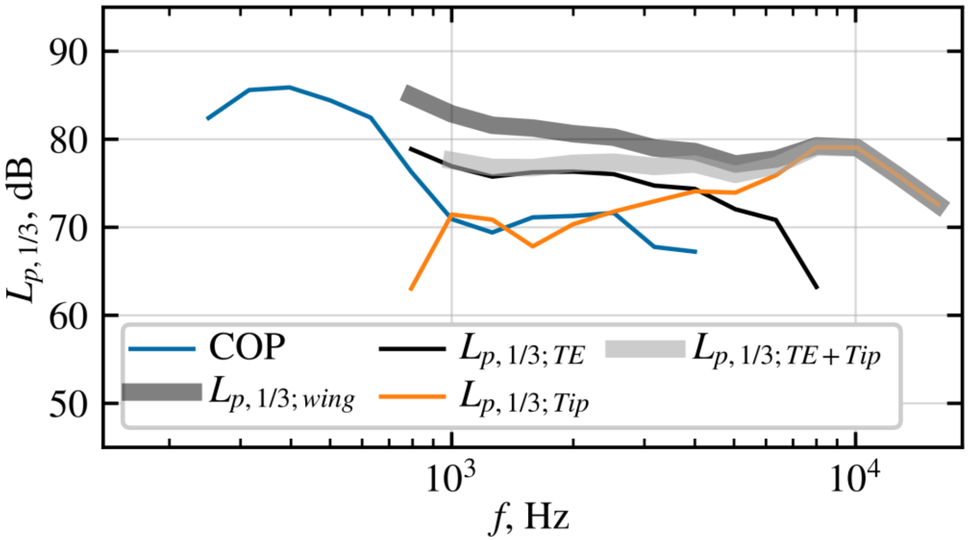

- $L_{p,1/3;Tip}$ and the installation noise are stronger from the last α.
- $L_{p,1/3;TE}$ increases in strength and is slightly downstream of the trailing edge in the source map.
- COP spectrum maximum shifts to 300 – 400 Hz.

Results

Source Localization, α= 20°

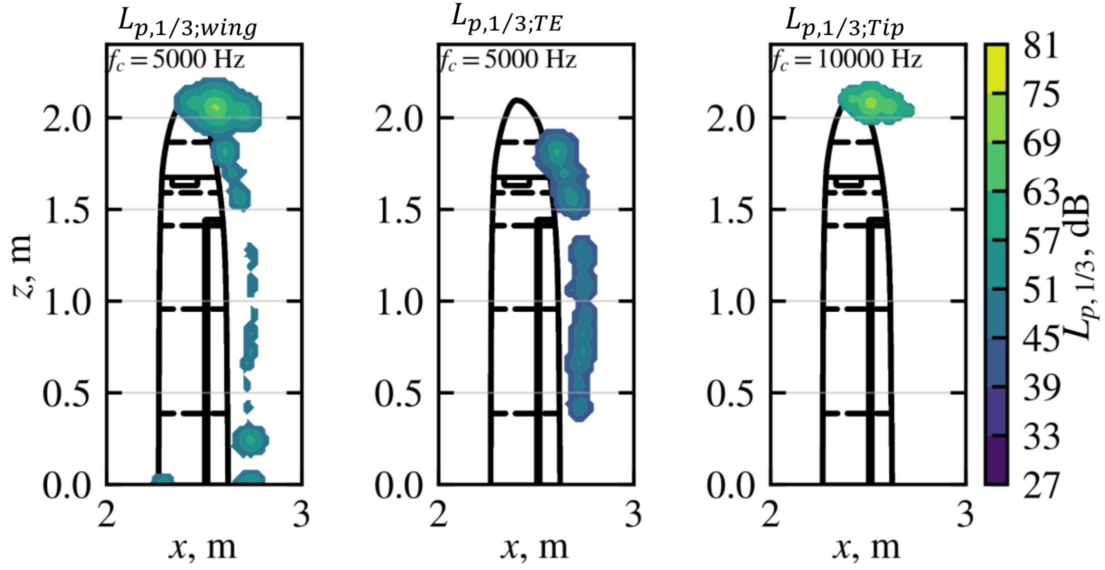

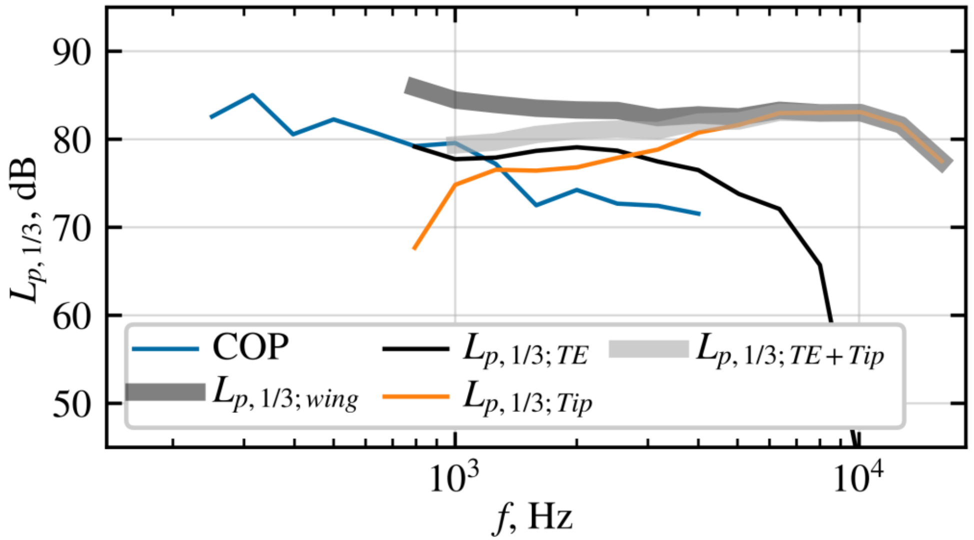

- $L_{p,1/3;Tip}$ also intensifies and is predominant from the mid to high-frequencies.
- $L_{p,1/3;TE}$ intensifies and further displaced downstream compared to the last α.
- At stall angle, COP spectrum does not show a clear peak.

Results

Mach Number Scaling

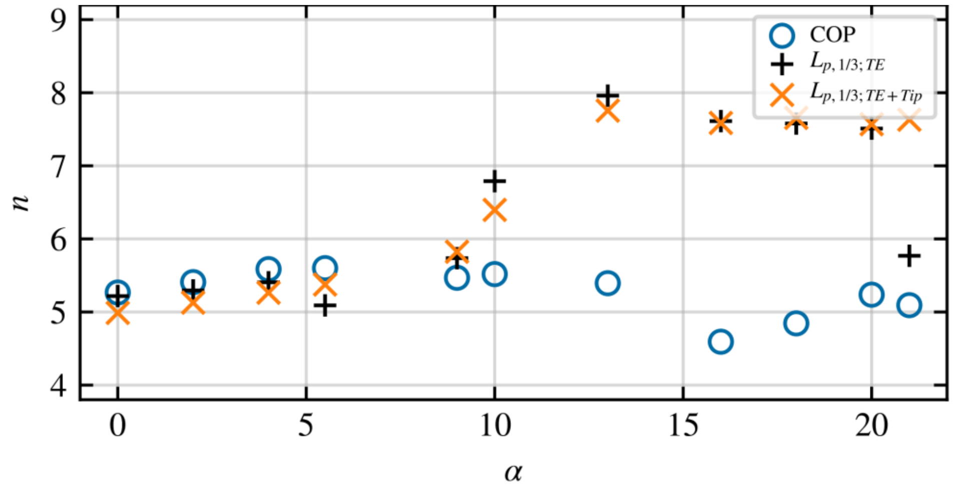

Coherent Output Power spectra, α= 10°

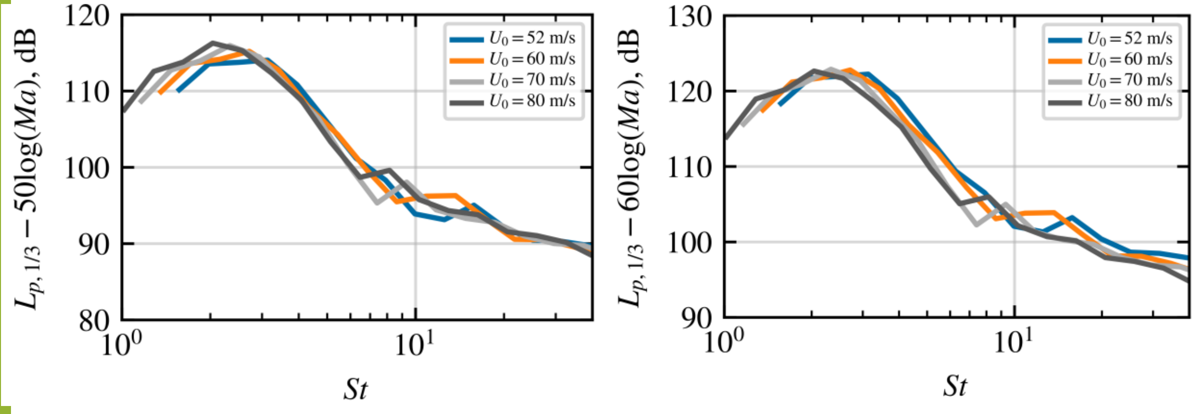

- Linear regression of $10\log(p'^2) \sim n \times 10\log(Ma)$.
- $L_{p,1/3;TE}$ scales with $n \approx 5$ for α< 8°and $n \approx 8$ for α> 13°
- COP spectrums scales with n=[4.5, 5.5]
  - A mixture of non-compact body radiation (Ma^5), St> 3, and compact body radiation (Ma^6), St< 3.
  - $St = f_c \, \bar{c}_a / U_0$
- Turner and Kim (2022), DNS of NACA 0012 at Re=50000 → Quadrupole noise sources due to the separated shear layers

Turner, Jacob M.; Kim, Jae Wook (2022): Quadrupole noise generated from a low-speed aerofoil in near- and full-stall conditions. In *J. Fluid Mech.* 936. DOI: 10.1017/jfm.2022.75.

Conclusions

- Acoustic measurement had been conducted for large Reynolds number flows for α=0° to stall.
- Evaluation using COP and phased-microphone array separates dipole and non-dipole sound sources.
- COP enables evaluation down to 200 Hz in the NWB.
- The COP overall sound pressure level scales with $Ma^{\approx 5}$. At large α, the acoustic radiation is a mixture of acoustically compact (St<3) and non-compact bodies (St>3).
- The mid-frequency range 800 Hz – 5 kHz scales with Ma^{5} for α<8° and Ma^{8} for α>13°
- Flow separation at large Reynolds numbers can lead to a mixture of dipole and quadrupole noise sources.

Perspectives:

- Comparison of flow separation noise model
- Evaluation of surface pressure fluctuations

Impressum

Thema: **Flow Separation Noise Sources**

Datum: 2024-11-13 (JJJJ-MM-TT)

Autor: Suryadi, Alexandre

Institut: AS-WEA

Bildcredits: Alle Bilder „DLR (CC BY-NC-ND 3.0)“, sofern nicht anders angegeben